Experimental investigation of the critical state of unsaturated silty sand from Beijing

G.Q. Cai [a,b], Saman Asreazad [a,b], C. Liu [a,b,c], Y.N. Wang [b], C.G. Zhao [a,b,d]

[a] *MOE Key Laboratory of Urban Underground Engineering, Beijing 100044, China*

[b] *School of Civil Engineering and Architecture, Beijing Jiaotong University, Beijing 100044, China*

[c] *Tianjin municipal engineering design and research institute, Tianjin 300051, China*

[d] *School of Civil Engineering and Architecture, Guilin University of Technology, Guilin Guangxi 541004, China*

ABSTRACT: Critical state models for unsaturated soils have been proposed in recent years. However, the corresponding experimental data are still very limited. This paper deals with the evaluation of the critical-state parameters with respect to the net stress, matric suction and density for saturated and unsaturated silty sand from Beijing. Suction-controlled triaxial drained shear tests on compacted soil specimens with different initial densities were carried out. The volume change of both soil specimen and water were measured during shearing. The critical state line equations on the planes of q-p', v-lnp' and v_w-lnp' are proposed. This experimental study has further demonstrated that matric suction has no influence on parameters of M and λ, while λ_w is dependent on suction.

1 INTRODUCTION

Since Schofield and Wroth (1968) proposed the critical state theory, the reaserch of the critical state of saturated soils has developed rapidly (Toll 1990; Wood 1991; Maatouk et al 1995; Adams 1997; Newson 1998). Based on research of saturated soils, many scholars have conducted experiments and theoretical studies for the critical state about unsaturated soils.

Toll et al. (2003) proposed functions of M_a, M_b and established the relationship with the parameters in the critical state equations of saturated soil. Wang et al. (2002) conducted triaxial tests by controlling the suction of silty soil and the results showed that the critical state lines of unsaturated soil are parallel with different suction values. Triaxial tests performed on Turkish residual clayey soil by Kayadelen et al. (2007) further verified that suction had no effect on the critical state parameters M and λ. Chen (2014) extrapolated the critical state model of unsaturated soil from the p-s plane to the triaxial stress space, assuming the slope of the critical state line did not change with the suction. Zhang (2015) conducted a drained triaxial shear test on Q3 intact loess by controlling the suction and net stress and the results showed that the effect of suction on the critical state line decreased as the net stress increased. Sheng (2011) presents a review of constitutive models for unsaturated soil focusing on the fundamental principles that govern the volume change, shear strength, water retention and hydro mechanical coupling. It is apparent that the critical state equation need further research in the determination of coefficient, especially for the effect of factors such as the types of soil, dry density of soil and the process of wetting-drying on the coefficient of critical state equation.

In addition, there are doubt about the choice of variables in the critical state of unsaturated soils. Wheeler et al. (1995) found that v_w did not reach a steady state at the critical state. In contrast, v_w measured by Ranpino et al. (1998) tended to be stable in the critical state. Therefore, Wang et al. (2002) suggested that more experimental data were needed to determine whether v_w could be treated as an independent variable in the critical state of unsaturated soils.

In this study, suction-controlled triaxial drained shear tests on unsaturated silty sand from Beijing with different initial densities were carried out in order to investigate the critical state behavior of the soil. The volume change of both soil specimen and water were measured during shearing. Based on the experimental data, the critical state line equations were proposed. The rationality of taking pore water ratio volume v_w as a critical state variable has also been verified.

2 TEST MATERIALS AND TESTING PROGRAM

2.1 *Test materials*

The silty sand empoyed in this study were obtained from the foundation pit of a station on Beijing Metro Line 16. Liquid limit, specific gravity and plasticity index are found to be 15.4%, 2.67 and 5.5%. The representative geotechnical properties are summarized in Table 1 and the particle size gradation curve is shown in Figure 1. The soil was remolded into cylindrical specimens with a diameter of 3.91 cm and a height of 8 cm. Figure 2 shows the compaction test curve.

Table 1. Physical properties of the soil specimens.

Dry density (g/cm^3)	Saturation degree (%)	Pore ratio	Specific gravity	Water content (%)
1.96	49.2	0.36	2.67	6.5
1.6	28.5	0.68	2.67	6.5

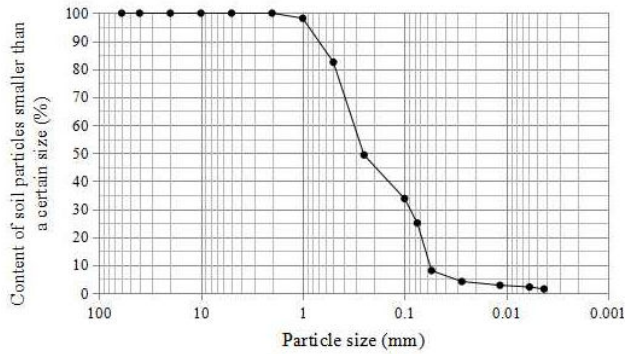

Figure 1. Gradation curve of the silty sand.

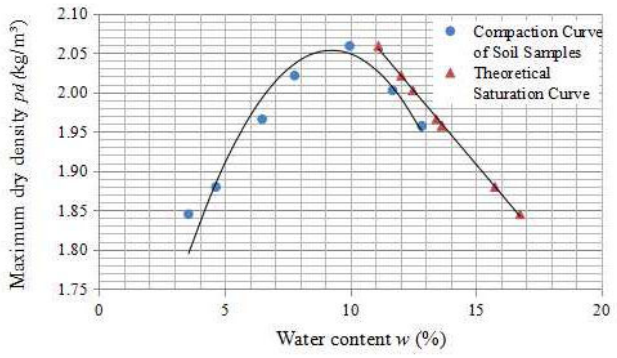

Figure 2. Compaction curve of the silty sand.

2.2 *The testing program*

The tests were performed on specimens with the initial dry densities, 1.6 g/cm^3 and 1.96 g/cm^3. In order to evaluate the critical states of unsaturated soils, the unsaturated triaxial test system was used to conduct the tests at suctions of 30 kPa, 100 kPa, and 200 kPa (corresponding net stresses were 100 kPa, 200 kPa, and 300 kPa, respectively) using axial translation technology.

The process can be grouped into three stages: equilibrium suction, consolidation at constant suction, and shearing at constant suction. During the equilibrium suction stage, the specimens were subjected to a net stress of 30 kPa and the pressure and back pressure were increased at a rate of 1.5 kPa/min to the pre-set value. The consolidation at constant suction was achieved by keeping the confining pressure constant while decreasing the air pressure and water pressure at a rate of 0.5 kPa/h. The constant-suction shearing applied to the specimens was strain controlled. The shear test was completed when the maximum shear strain was 30% (24 mm), or the deviatoric stress and volume deformation reached a relatively stable value. The program are shown in Tables 2, 3 and 4 and the stress paths are shown in Figures 3 and 4. In the tables, the specimen number consists of the series number (S30, S100, S200, S300) followed by a number representing the net pressure, (σ_c - u_a), where σ_c is the radial stress or confining pressure.

Table 2. Testing program for the equilibrium suction stage.

Test number	σ_c	u_a	u_w	$\sigma_c - u_a$	$s = u_a - u_w$
S30-100	550	520	490	30	30
S30-200	550	520	490	30	30
S30-300	550	520	490	30	30
S100-100	550	520	420	30	100
S100-200	550	520	420	30	100
S100-300	550	520	420	30	100
S200-100	550	520	320	30	200
S200-200	550	520	320	30	200
S200-300	550	520	320	30	200

Table 3. Testing program for the consolidation stage.

Test number	σ_c	u_a	u_w	$\sigma_c - u_a$	$u_a - u_w$
S30-100	550	450	420	100	30
S30-200	550	350	320	200	30
S30-300	550	250	220	300	30
S100-100	550	450	350	100	100
S100-200	550	350	250	200	100
S100-300	550	250	150	300	100
S200-100	550	450	250	100	200
S200-200	550	350	150	200	200
S200-300	550	250	50	300	200

Table 4. Testing program for the shear stage.

Test number	σ_c	u_a	u_w	$\sigma_c - u_a$	$u_a - u_w$
S30-100	550	450	420	100	30
S30-200	550	350	320	200	30
S30-300	550	250	220	300	30
S100-100	550	450	350	100	100
S100-200	550	350	250	200	100
S100-300	550	250	150	300	100
S200-100	550	450	250	100	200
S200-200	550	350	150	200	200
S200-300	550	250	50	300	200

For the saturated silty sands of different initial dry densities, triaxial shear tests under different net stresses (100 kPa, 200 kPa, 300 kPa and 400 kPa) were also conducted.

The triaxial shear tests of the saturated silty sand consisted of three stages: backpressure saturation, consolidation, and shear. To achieve a relatively high degree of saturation, the specimen was first vacuum saturated before installed in the pressure chamber. The shear was applied at a relatively low rate (0.015 mm/min) to ensure the specimens reached the critical state smoothly. The testing program are shown in Table 5. In the table, Δu_w is the back pressure, and $\Delta u_{w,max}$ is the upper limit value of the applied back pressure during the saturation.

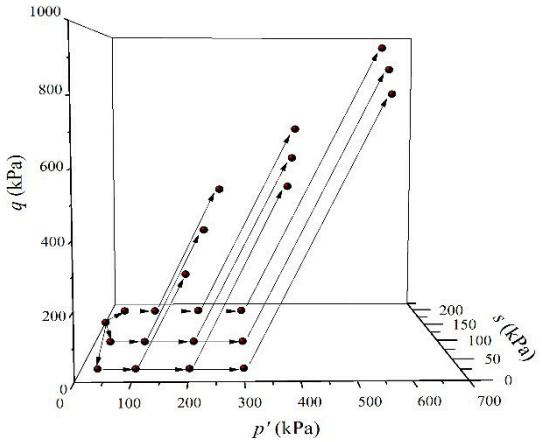

Figure 3. Stress paths of test specimens with a dry density of 1.6 g/cm^3.

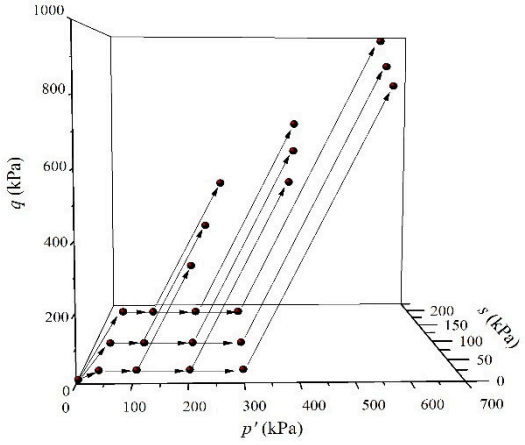

Figure 4. Stress paths of test specimens with a dry density of 1.96 g/cm3.

Table 5. Testing program for saturated soil triaxial shear.

Confining pressure	Back pressure saturation		Consolidation		Shear	
	Δu_w	$u_{w,max}$	σ_c	u_w	σ_c	u_w
100	30	300	400	300	400	300
200	30	300	500	300	500	300
300	30	300	600	300	600	300
400	30	300	700	300	700	300

3 RESULTS AND DISCUSSIONS

By conducting the triaxial shear tests of the saturated and unsaturated silty sand with dry densities of 1.6 g/cm³and 1.96 g/cm³ under the different suction and net stress values, the relationships between the deviatoric stress q (σ_1-σ_3), the volume strain ε_v and the axial strain ε_1 are shown in Figures 5-8. Based on the q-ε_1 and ε_v-ε_1 curves of the specimens, the test curves can be divided into hardening and softening types. The research about the effect of density on the critical state will be described and discussed in this context.

(1) The first diagrams in Figure 5, 6, 7 and 8 show the stress-strain curves of saturated soils with dry densities of 1.6 g/cm^3 and 1.96 g/cm^3 respectively. The deviatoric stress and volume strain increases with axial strain and reaches a maximum value or stable value at an axial strain range between 10 and 15%, indicating a critical state. The loading was terminated when the axial strain was about 20%. However, the specimens with the higher dry density bulged at failure and no distinct shearing planes were observed in first diagrams in Figure 7 and 8.

(2) The rest of the diagrams in Figure 5 , 6, 7 and 8 show the stress and strain curves of the unsaturated specimens (s = 30 kPa, 100 kPa, and 200 kPa) with dry densities of 1.6 g/cm^3 and 1.96 g/cm^3, respectively. For the same net stress, the strength of the unsaturated specimens is clearly greater than the strength of the saturated specimen. And a lower shear rate and a larger axial strain are required for the unsaturated specimens to reach the critical state.

(3) By contrast, the unsaturated specimens with 1.6 g/cm^3 dry density display typical shear characteristic of loose sand. The strength and volume increases to a stable value with the axial strain. However, the specimens with 1.96 g/cm^3 dry density display the typical shear characteristic of dense sand. The strength increases as the axial strain and then decrease after reaching the peak value. The volume first contracts and then expands. The saturated specimen with 1.96 g/cm^3 dry density no behave the such behavior and which demonstrates that suction strengthens the mechanical properties with given density specimens.

Based on the results discussed above, the average net stress, $p'=q/3+(\sigma_c-u_a)$, deviator stress, q, specific volume, v, and specific water volume, v_w, are measured at critical state for saturated and unsaturated specimens with each matric suction. And the critical state lines are shown in the q-p', v-lnp' and v_w-lnp' planes in Figures 9, 10 and 11.

(1) Figure 9 shows the critical state values in the q-p' space. As seen from figures, the unsaturated critical state line are found to be approximately parallel to the saturated line for each suction and moving downward in parallel as the suction decreases. The equations can be expressed as follows:

$$q = M \cdot p' + \mu(s) \tag{1}$$

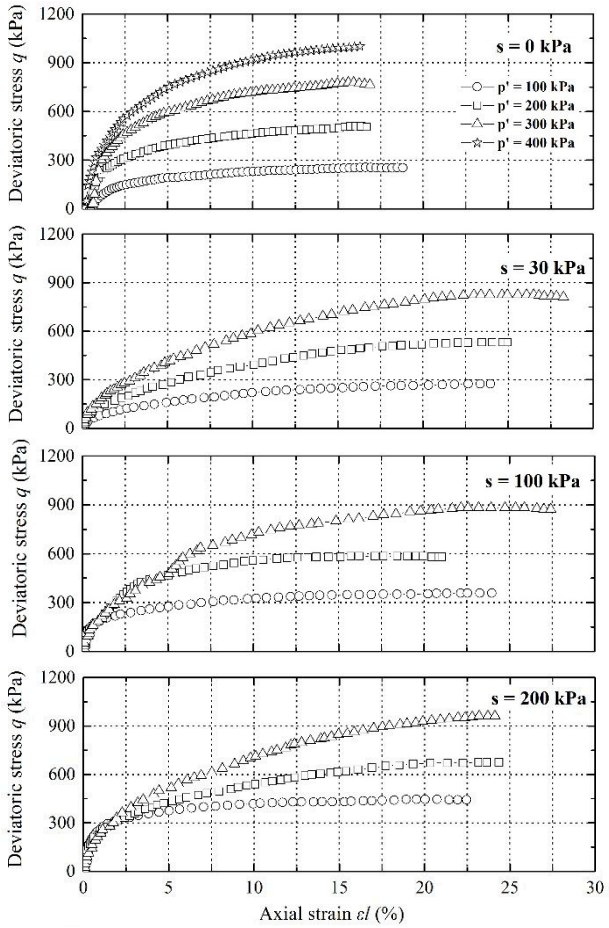

Figure 5. Stress curves of unsaturated silty sand under various suction conditions (ρ_d = 1.6 g/cm^3).

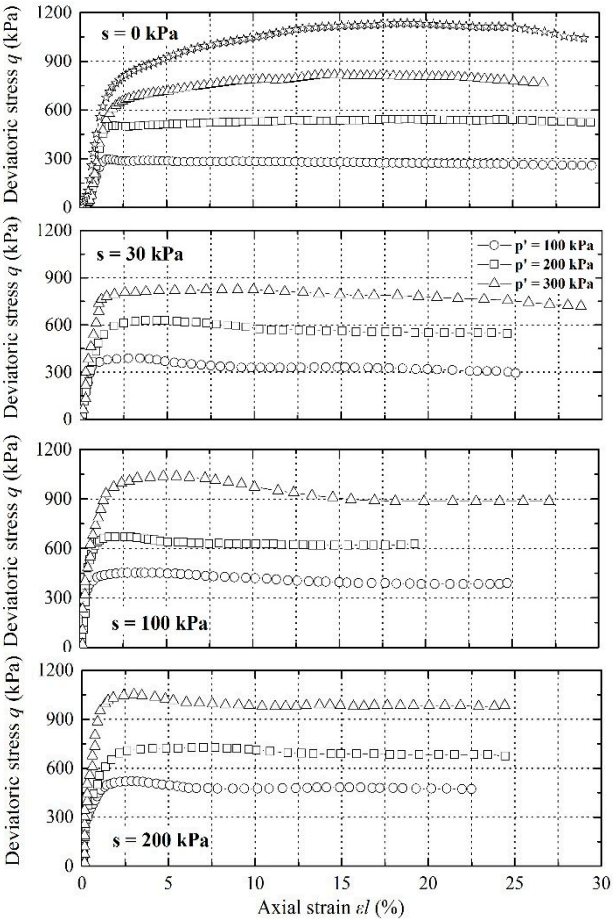

Figure 7. Stress curves of unsaturated silty sand under various suction conditions (ρ_d = 1.96 g/cm^3).

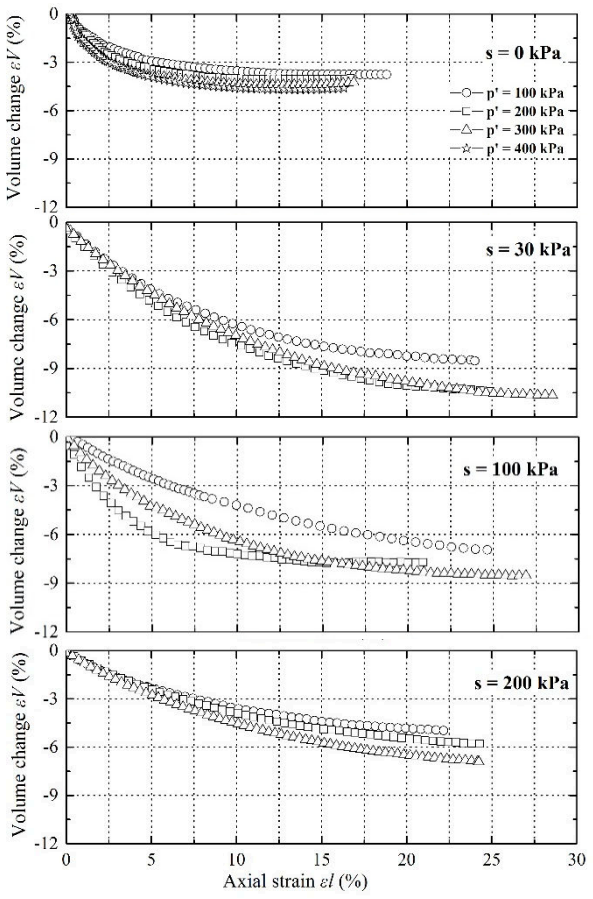

Figure 6. Strain curves of unsaturated silty sand under various suction conditions (ρ_d = 1.6 g/cm^3).

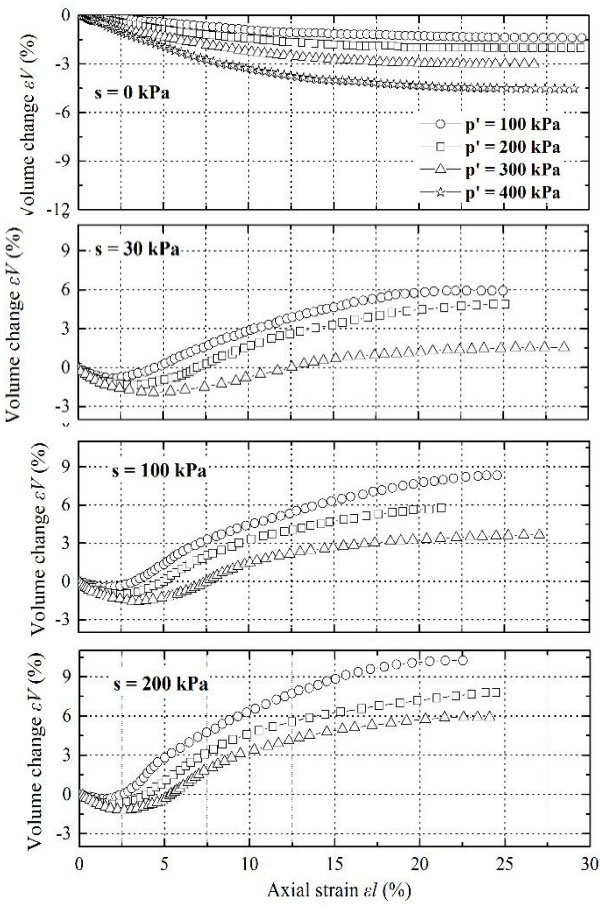

Figure 8. Strain curves of unsaturated silty sand under various suction conditions (ρ_d = 1.96 g/cm^3).

$$\mu(s) = -0.0004 \cdot s^2 + 0.5702 \cdot s + 0.6685 \quad (2)$$

$$\mu(s) = -0.0013 \cdot s^2 + 0.7976 \cdot s + 0.1129 \quad (3)$$

where M is the slope and determined from the saturated critical state line. The $\mu(s)$ is the intercept and dependent on suction. The $\mu(s)$ of 1.6 g/cm^3 and 1.96 g/cm^3 are given by equations (2) and (3), respectively.

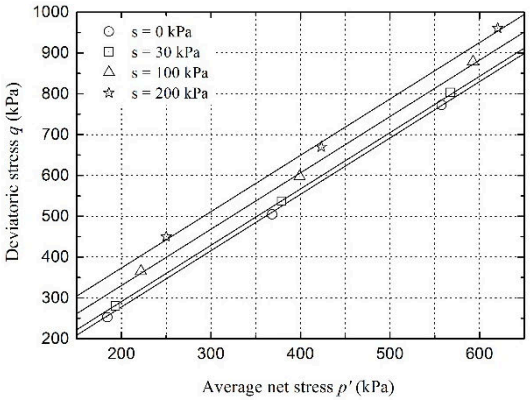

(a) ρ_d = 1.6 g/cm^3.

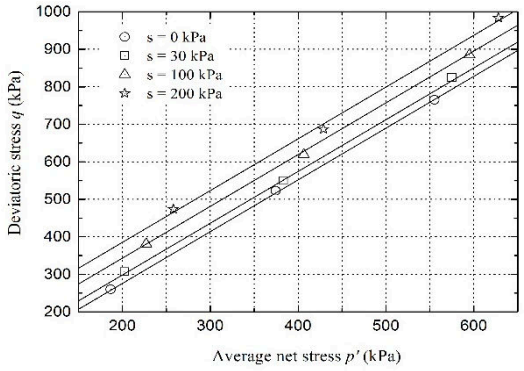

(b) ρ_d = 1.96 g/cm^3.

Figure 9. Critical state lines in the q-p' plane

(2) The characteristics of the critical states in the v-ln$p$' plane, shown in the Figure 10, are similar to the q-p' plane. The equations are:

$$v = \Gamma(s) - \lambda \cdot \ln(p') \quad (4)$$

$$\Gamma(s) = -1\mathrm{E}-06 \cdot s^2 + 0.0006 \cdot s + 1.8422 \quad (5)$$

$$\Gamma(s) = -1\mathrm{E}-06 \cdot s^2 + 0.0006 \cdot s + 1.7711 \quad (6)$$

where λ is the slope and similar to the saturated critical state. The $\Gamma(s)$ is intercept and dependent on suction. The $\Gamma(s)$ of 1.6 g/cm^3 and 1.96 g/cm^3 are given by equations (5) and (6), respectively.

(3) Changes in the pore water volume ratio, v_w=(1+wG$_s$), are shown in Figure 11. The values can also be fitted to a straight line in the v_w-ln$p$' plane and the intercept and slope can be expressed as $\Gamma(s)$, λ. However, those lines no display the parallel relationship just like in the q-p' and v-ln$p$' planes.

Based on the test results, we assume that the specimens reach the critical shear state and the state variable v_w reaches the final equilibrium state.

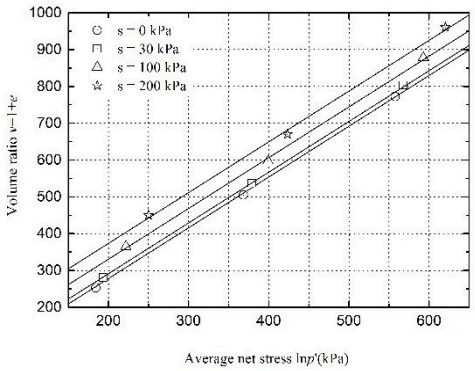

(a) ρ_d = 1.6 g/cm^3

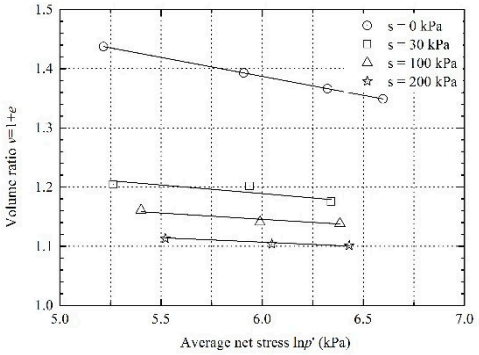

(b) ρ_d = 1.96 g/cm^3

Figure 10. Critical state lines in the v_w-ln$p$' plane

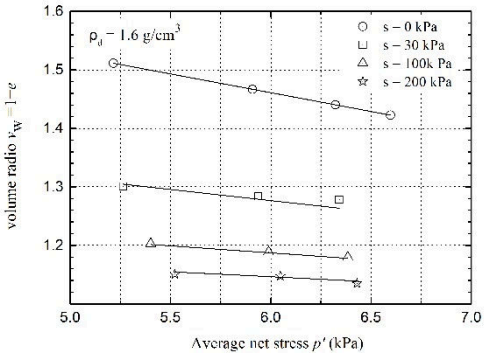

(a) ρ_d = 1.6 g/cm^3.

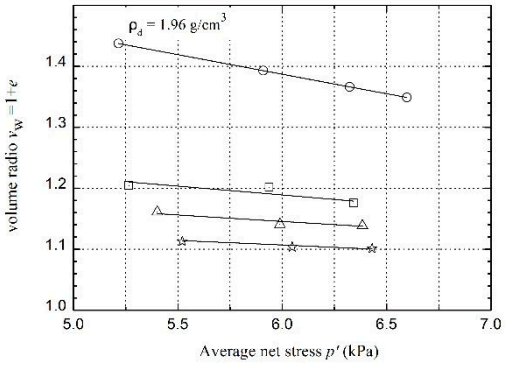

(b) ρ_d = 1.96 g/cm^3.

Figure 11. Critical state lines in the v_w-ln$p$' plane.

$$v_w = 1 + w \cdot G_s \quad (7)$$

$$v = 1 + e \quad (8)$$

$$S_r = \frac{w \cdot G_s}{e} \quad (9)$$

$$v = \Gamma(s) - \lambda \cdot \ln p' \quad (10)$$

According to equations (7) through (10), the critical state line could be expressed in terms of Γ_w and λ_w and requires three parameters, Γ, λ and S_r.

$$v_w = \Gamma_w - \lambda_w \cdot \ln p' \tag{11}$$

$$\Gamma_w = \Gamma(s) \cdot S_r - S_r + 1 \tag{12}$$

$$\lambda_w = S_r \cdot \lambda \tag{13}$$

The parameters in this study summarized in Table 6. Figure 11 shows the theoretical critical state line in the v_w-ln$p$' plane and shows good agreement with the test results, confirming the validity of the pore water ratio volume v_w as the critical state parameter.

Table 6 Parameters obtained from use of the critical state line equation in the v_w-ln$p$' plane.

ρ_d	s	S_r	λ	Γ(s)	λ_w	Γ_w
1.6 g/cm³	0	1	0.064	1.845	0.064	1.8450
	30	0.62		1.855	0.040	1.5301
	100	0.37		1.895	0.024	1.3312
	200	0.27		1.92	0.017	1.2484
1.96 g/cm³	0	1	0.064	1.771	0.064	1.7710
	30	0.46		1.789	0.029	1.3629
	100	0.33		1.823	0.021	1.2716
	200	0.23		1.856	0.015	1.1969

4 CONCLUSIONS

The triaxial test on saturated and unsaturated silty sand were carried out. The silty sand, remolded to different densities, was subjected to different net stress and suction conditions and were sheared to the critical state. Soil strength, volume deformation and degree of saturation were observed. Based on the experimental data, the conclusions can be obtained as follow:

(1) The saturated silty sand bulges in the critical shear state, but a distinct shear failure surface does not develop. Compared with the saturated soil, a lower shear rate and a larger axial strain are required for the unsaturated silty sand to reach a critical shear state.

(2) The triaxial tests of the unsaturated soils show that, at a given net stress, the strength increases as the suction increases. Under a given suction, the strength also increases as the net stress increases. Under a given net stress, as the suction increases, smaller compression of volume strain results in greater expansion. Under a given suction condition, as the net stress increases, greater compression results in lesser expansion.

(3) The slope M of the critical state line of the unsaturated soil in the q-p' plane is not affected by the suction and equal to the saturated soil. The intercept μ is a function of the suction. The slope λ in the v-ln$p$' plane is equal to the saturated soil and the intercept Γ is a function of the suction. The slope λ_w and intercept Γ_w of the critical state line of the unsaturated soil in the v_w - ln$p$' plane is the function of the saturation degree and the coefficients of the function are λ and Γ.

5 ACKNOWLEDGMENTS

The research is supported by the National Natural Science Foundation of China (51722802,51678041), Beijing Municipal Natural Science Foundation (8162032) , the Fundamental Research Funds for the Central Universities (2017JBM091) and the Research Funds for Henan transportation department (2017B4).

6 REFERENCES

Adams, B.A., & Wulfsohn, D. 1997. Nariation of the critical-state boundaries of an agriculture soil. *European Journal of Soil Science* 48(4): 739-758.

Chen, Z.H. 2014. On basic theories of unsaturated soils and special soils. *Chinese Journal of Geotechnical Engineering.* 36(2): 201-272. (in Chinese)

Kayadelen, C. Sivrikaya, O. & Taskiran, T. 2007. Critical-state parameters of an unsaturated residual clayey soil from Turkey. *Engineering Geology* 94(1-2): 1-9.

Maatouk, A., Leroueil, S., & ROCHELLE, P.L.A. 1995. Yielding and critical state of a collapsible unsaturated silty soil. *Géotechnique* 45(3): 465-477.

Newson, T.A. 1998. Validation of a non-associated critical state mode. *Computers and Geotechnics* 23(4):277-287.

Rampino, C., Mancuso, C., & Ninale, F. 1998. Behavior of a compacted silty sand during suction controlled tests. *Proceedingds of the 2nd International Conference on Unsaturated Soils* 1: 108-113.

Schofield, A.N. & Wroth, P. 1968. *Critical State Soil Mechanics* 7(70): 23-56.

Sheng, D.C. 2011. Review of fundamental principles in modelling unsaturated soil behavior. *Computers and Geotechnics* 38: 757-776.

Toll, D.G. 1990. A framework for unsaturated soil behavior. *Géotechnique* 40(1): 31-44.

Toll, D.G., & Ong, B.H. 2003. Critical-state parameters for an unsaturated residual sandy clay. *Géotechnique* 53(1): 93-104.

Wang, Q., Pufahl, D.E., & Fredlund, D.G. 2002. A study of critical state on an unsaturated silty soil. *Canadian Geotechnical Journ*al 39: 213-218.

Wheeler, S.J., & Sivakumar, N. 1995. An elasto-plastic critical state framework for unsaturated soil. *Géotechnique* 45(1): 35-53.

Wood, D.M. 1991. *Soil behaviour and critical state soil mechanics*. Cambridge university press.

Zhang, D.F., CHEN, C.l., & LI, W.W. 2015. Characteristics of critical state and water volume change for Q3 unsaturated intact loess. *Chinese Journal of Geotechnical Engineering* 37(s1):197-201. (in Chinese)